Advanced Composite Materials
Publication details, including instructions for authors and subscription information:
http://www.tandfonline.com/loi/tacm20

Modeling of push-out test for interfacial fracture toughness of fiber-reinforced composites

M.N. Yuan [a b] , Y.Q. Yang [b] & Z.H. Xia [c]

[a] Department of Mechanical and Electrical Engineering, College of Mechanical and Electrical Engineering, North University of China, Taiyuan, 030051, P.R. China

[b] Department of Materials Science and Engineering, School of Material, Northwestern Polytechnical University, Xi'an, 710072, P.R. China

[c] Department of Mechanical Engineering, University of Akron, Akron, 44325, OH, USA

Version of record first published: 26 Oct 2012.

To cite this article: M.N. Yuan , Y.Q. Yang & Z.H. Xia (2012): Modeling of push-out test for interfacial fracture toughness of fiber-reinforced composites, Advanced Composite Materials, 21:5-6, 401-412

To link to this article: http://dx.doi.org/10.1080/09243046.2012.738631

Advanced Composite Materials
Vol. 21, Nos. 5–6, October–December 2012, 401–412

Modeling of push-out test for interfacial fracture toughness of fiber-reinforced composites

M.N. Yuan[a,b], Y.Q. Yang[b] and Z.H. Xia[c]*

[a]*Department of Mechanical and Electrical Engineering, College of Mechanical and Electrical Engineering, North University of China, Taiyuan 030051, P.R. China;* [b]*Department of Materials Science and Engineering, School of Material, Northwestern Polytechnical University, Xi'an 710072, P.R. China;* [c]*Department of Mechanical Engineering, University of Akron, Akron 44325, OH, USA*

(*Received 24 January 2010; accepted 6 September 2012*)

An analytical model of the push-out test was developed to predict the interfacial fracture toughness of fiber-reinforced matrix composites. Elastic deformation, thermal residual stress, Poisson effect, and energy dissipation due to interfacial friction are all accounted for in the model based on a fracture mechanics approach and a general solution was derived from the analysis. In addition, finite element analysis was performed to validate the analytical model. The results show that the predictions from the analytical model are in good agreement with the finite element results and experimental data on SiC-reinforced Timetal834 composites. The effects of residual stress, the friction stress ,and the debonding crack length on the interfacial fracture toughness were discussed for a better understanding of the interfacial phenomena in push-out test. The analytical model could be applied to other composite systems as well.

Keywords: metal matrix composites; shear lag model; interfacial fracture toughness push-out

1. Introduction

Fiber-reinforced composites, such as SiC/Ti composites, are being considered as a potential material system of choice for the advanced propulsion systems of aircrafts, owing to their high specific strength and high toughness. One of the critical issues in the successful application of the fiber-reinforced composites is the fiber/matrix interface that determines the mechanical properties of the composites [1–4]. To date, much effort has been made to understand the interfacial behaviors and evaluate the interfacial strength experimentally. Various techniques, such as the pull-out test [5], the push-out test [6], and the fragmentation test [7], have been developed to measure the interfacial properties. Among these techniques, the fiber push-out test is one of the most popular methods as it is simple to perform and the specimens are easy to prepare. In the push-out test, the values of shear strength and frictional shear stress are evaluated by average. Since the stress distribution in push-out test is complex due to edge effect or crack growth during the push-out test [8], the average values do not represent the real behavior of the interfaces and may mislead in some cases. It is, therefore, necessary to carefully model the push-out process so as to interpret the unusual phenomena in the push-out tests and further accurately extract the interfacial properties of the composites.

*Corresponding author. Email: zxia@uakron.edu

ISSN 0924-3046 print/ISSN 1568-5519 online

http://dx.doi.org/10.1080/09243046.2012.738631
http://www.tandfonline.com

Several analytical models have been developed to study the push-out test [9–13]. Basically, there are two approaches to determine the interfacial properties. One is the maximum shear stress criterion that the debonding occurs when the interfacial shear stress exceeds the interfacial shear strength. The other one is the interfacial fracture toughness criterion based on the concept of fracture mechanics where the debonding region is considered as an interfacial crack and its propagation is dependent on the energy balance in terms of the interface fracture toughness. Although the former approach is relatively simple, the approach based on fracture mechanics is increasingly being considered as a more appropriate quantitative measure of the bond strength of the interface. Majumdar and Miracle [14] used the latter approach to evaluate the interfacial fracture toughness of SiC/Ti composites, yielding a value of about $30\,J/m^2$. However, in their analysis, thermal strain energy and the strain energy dissipated by friction stress were ignored. Kalton et al. [15] considered the strain energy dissipated by friction stress in their model based on Majumdar's work but the contribution of the thermal strain energy to the interfacial fracture toughness was still missing. Since the thermal stress in high-temperature composite materials is usually high, at the level of several hundred mega Pascals [16], it is likely that the thermal stress significantly affects the stress distribution during push-out test and further evaluation of the interfacial fracture toughness. Indeed, the interfacial fracture toughness of Ti-6AL-4 V/Sigma-1240 predicted by Kalton et al. without considering the thermal stress is $10\,J/m^2$, much smaller than the results from finite element analysis [1,17].

In this paper, an analytical model has been developed to predict the interfacial fracture toughness of fiber-reinforced composites, in which all possible sources that affect the push-out process, including mechanical, thermal, friction dissipation, and the Poisson effect are accounted for. A finite element model of the push-out test was also developed to validate the analytical model. The models were applied to SiC/Timetal-834 composite materials to predict the interfacial fracture toughness. It is shown that the interfacial fracture toughness predicted by the analytical model is in good agreement with the results from the finite element analysis and experimental data. This work provides a new insight into the interfacial failure mechanisms and the role of the interface in determining the mechanical properties.

2. The analytical model and solution for push-out test

2.1. The push-out model

The model considered in this study, schematically shown in Figure 1, is a unidirectional fiber-reinforced composite consisting of a cylindrical fiber of radius r_f, length L, Young's modulus E_f, and Poisson ratio ν_f, embedded in a matrix material. A set of cylindrical coordinates (r, θ, and z) is set so that the z-axis corresponds to the axis of the fiber and r is the radial distance from the fiber axis. A compressive stress σ_p is applied to the top free end ($z=0$) of the fiber, and the matrix is fixed at the bottom end $z=L$. We assume that the stress in the fiber is independent of radial location. For high-temperature composite materials, the matrix–fiber mismatch usually introduces high thermal residual stresses in the matrix and the fibers. These residual stresses cause the nanotube/matrix interface debonding close to the free surface of the composite specimens before push-out testing. To consider this end effect, an initial crack with a crack length of a_0 is introduced in this model. During the push-out testing, the propagation of the interface crack (a) is assumed to start only from the supported end. After debonding, a constant frictional stress τ is assumed along the fiber/matrix interface.

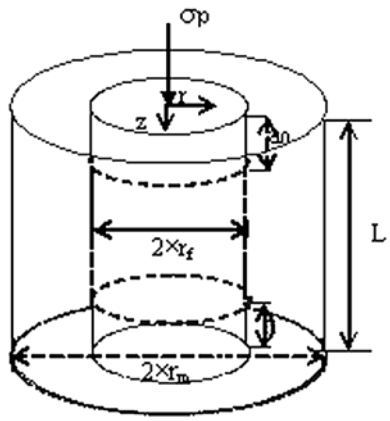

Figure 1. A fiber–matrix model of the push-out test.

2.2. *Analytical solution to interfacial fracture toughness*

From the concept of fracture mechanics, interfacial debonding occurs when the potential energy change in the system with respect to the debonding crack extension a is equal to the interfacial fracture toughness G_{Ic} [9]

$$G_{\mathrm{Ic}} = \frac{1}{2\pi r_{\mathrm{f}}} \frac{\mathrm{d}U}{\mathrm{d}a} \tag{1}$$

where, $\mathrm{d}U$ is the change in total strain energy stored in the specimen. Since the total strain energy change $\mathrm{d}U$ is caused by thermal residual stress σ_{fr} [17,18], applied stress σ_{p}, and interface friction stress τ [13,19], U can be decomposed into three parts: (i) the strain energy U_{P} due to the applied stress, (ii) the residual strain energy U_{R} due to thermal residual stress, and (iii) the strain energy dissipated by friction stress U_{F}. Thus, interfacial fracture toughness can be rewritten as:

$$G_{\mathrm{Ic}} = \frac{1}{2\pi r_{\mathrm{f}}} \left(\frac{\mathrm{d}U_{\mathrm{P}}}{\mathrm{d}a} + \frac{\mathrm{d}U_{\mathrm{R}}}{\mathrm{d}a} - \frac{\mathrm{d}U_{\mathrm{F}}}{\mathrm{d}a} \right) \tag{2}$$

The strain energy can be obtained by integrating strain energy density ($\frac{1}{2}\sigma\varepsilon$) over the volume of specimen. Since the strain energy change in matrix is small, it can be safely neglected [15]. The total strain energy due to the applied stress U_{P} in the specimen can be written as:

$$U_{\mathrm{P}} = \int_0^L \frac{1}{2} \sigma_{\mathrm{f}} \varepsilon_{\mathrm{f}} \, \mathrm{d}V \tag{3}$$

where, σ_{f} and ε_{f} are the axial stress and strain in the fiber, respectively.

In the push-out test, the specimen can be divided into five regions according to the axial stress distribution in the fiber, as schematically shown in Figure 2. In Regions I and V, the interfaces are debonded, resulting in thermal residual stress redistribution and a constant frictional stress. Regions II and IV are in front of the cracks, where the stress distribution changes abruptly but it will not be affected significantly by the interfacial crack propagation. It is, therefore, reasonable to assume that the strain energy is neglected in these small regions [14]. In Region III, the axial stress in the fiber is constant while the frictional stress is zero. For Regions I and V, the axial forces in the fiber are in equilibrium and can be described by

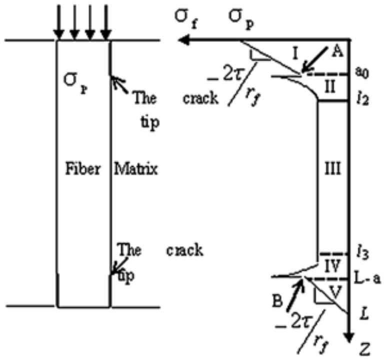

Figure 2. Schematic representation of the axial stress in the fiber during push-out test.

$$\frac{d\sigma_f(z)}{dz} = -\frac{2}{r_f}\tau(z) \tag{4}$$

where, $\sigma_f(z)$ is the axial stress in the fiber at the axial position z. Integrating Equation (4) over Region I, we have the axial stress $\sigma_I = \sigma_P - \frac{2\tau}{r_f}z$. Similarly, the axial stress in Region V is $\sigma_V = \frac{2\tau}{r_f}(L-z)$. In Region III, the axial stress in the fiber is $\sigma_{III} = \sigma_P - \sigma_{fr}^z - \frac{2\tau}{r_f}a_0$, where a_0 is the length of Region I and σ_{fr}^z is the axial thermal residual stress in the fiber. From above analysis, the total strain energy U_P can be expressed as:

$$U_P = \int_0^{a_0} \frac{1}{2}\,\sigma_I(z)\varepsilon_I(z)\;dV + \int_{l_2}^{l_3} \frac{1}{2}\,\sigma_{III}(z)\varepsilon_{III}(z)\;dV + \int_{L-a}^{L} \frac{1}{2}\,\sigma_v(z)\varepsilon_V(z)\;dV \tag{5}$$

For elastic deformation, the relationship between strain and stress is given by:

$$\varepsilon_f^z(r,z) = \frac{1}{E_f}\left\{\sigma_f^z(r,z) + v_f\left[\sigma_{fr}^r(r,z) + \sigma_{fr}^\theta(r,z)\right]\right\} \tag{6}$$

where, σ_{fr}^r and σ_{fr}^z are radial and tangential thermal residual stress in the fiber, respectively Assuming that the radial thermal residual is equal to the tangential thermal residual [20], i.e. $\sigma_{fr}^r(z) = \sigma_{fr}^\theta(z)$, Equation (6) can be rewritten as:

$$\varepsilon_f^z(r,z) = \frac{1}{E_f}\left\{\sigma_f^z(r,z) + 2v_f\sigma_{fr}^r(r,z)\right\} \tag{7}$$

Substituting Equation (7) and $dV = \pi r^2\;dz$ into Equation (5), we have

$$\begin{aligned} U_P = \tfrac{\pi r_f^2}{2E_f}\textstyle\int_0^{a_0}\left[\sigma_1(z)^2 + 2\upsilon\sigma_1(z)\sigma_{fr}^r(r,z)\right]dz + \int_{l_2}^{l_3}\left[\sigma_{111}(z)^2 + 2v\sigma_{111}(z)\sigma_{fr}^r(r,z)\right]dz \\ + \textstyle\int_{L-a}^{L}\left[\sigma_V(z)^2 + 2\upsilon\sigma_V(z)\sigma_{fr}^r(r,z)\right]dz \end{aligned} \tag{8}$$

Differentiating Equation (8) with respect to crack length yields:

$$\frac{dU_P}{da} = \frac{\pi r_f^2}{2E_f}\left[\left(\sigma_p - \frac{2\tau a_0}{r_f} - \sigma_{fr}^z\right)^2 + 2\upsilon\left(\sigma_p - \frac{2\tau a_0}{r_f} - \sigma_{fr}^z\right)\sigma_{fr}^r - \left(\frac{2\tau a}{r_f}\right)^2 - \frac{4\upsilon\tau a}{r_f}\sigma_{fr}^r\right] \tag{9}$$

Similarly, the residual strain energy is expressed as follows:

$$U_{\mathrm{R}} = \int_0^L \frac{1}{2}\,\sigma_{\mathrm{fr}}^z \varepsilon_{\mathrm{fr}}^z \mathrm{d}V + \int_0^L \frac{1}{2}\,\sigma_{\mathrm{fr}}^{\mathrm{r}} \varepsilon_{\mathrm{fr}}^{\mathrm{r}} \mathrm{d}V \tag{10}$$

where, $\varepsilon_{\mathrm{fr}}^{\mathrm{r}}$ and $\varepsilon_{\mathrm{fr}}^{z}$ are radial and axial residual strain in the fiber, respectively. The increase in residual strain energy with crack length is expressed as:

$$\frac{\mathrm{d}U_{\mathrm{R}}}{\mathrm{d}a} = \frac{\pi r_{\mathrm{f}}^2}{2E_{\mathrm{f}}}\left((\sigma_{\mathrm{fr}}^z)^2 + (\sigma_{\mathrm{fr}}^{\mathrm{r}})^2\right) \tag{11}$$

The strain energy dissipated by interfacial frictional stress is analyzed as follows:

$$U_{\mathrm{f}} = \int_{L-a}^{L} \frac{1}{2}\tau\varepsilon_i^{\mathrm{f}} \mathrm{d}V \tag{12}$$

$\varepsilon_i^{\mathrm{f}}(z)$ in Equation (12) can be expressed as

$$\varepsilon_i^{\mathrm{f}}(z) = \int_{L-a}^{z} (\varepsilon_{\mathrm{final}} - \varepsilon_{\mathrm{initial}})\mathrm{d}z \tag{13}$$

where, $\varepsilon_{\mathrm{final}} = \left(\sigma_{\mathrm{P}} - \frac{2\tau}{r_{\mathrm{f}}}a_0 - \sigma_{\mathrm{fr}}^z\right) \times \frac{1}{E_{\mathrm{f}}}$ and $\varepsilon_{\mathrm{initial}} = \frac{2\tau}{E_{\mathrm{f}} r_{\mathrm{f}}}(L - z)$. Substituting $\varepsilon_{\mathrm{initial}}$ and $\varepsilon_{\mathrm{final}}$ into Equation (13) and integrating it, we have:

$$\varepsilon_i^{\mathrm{f}}(z) = \frac{1}{E_{\mathrm{f}}}\left[\left(\sigma_{\mathrm{p}} - \frac{2\tau a_0}{r_{\mathrm{f}}} - \sigma_{\mathrm{fr}}^z\right) \times (z - L + a) + \frac{\tau}{r_{\mathrm{f}}}\left((L-z)^2 - (a)^2\right)\right] \tag{14}$$

Substituting Equation (14) into (12), we have the strain energy dissipated by interfacial friction stress:

$$U_{\mathrm{fr}} = \frac{2\pi r_{\mathrm{f}}}{E_{\mathrm{f}}}\int_{L-a}^{L} \tau\left[\left(\sigma_{\mathrm{P}} - \frac{2\tau a_0}{r_{\mathrm{f}}} - \sigma_{\mathrm{fr}}^z\right)(z - L + a) + \frac{\tau}{r_{\mathrm{f}}}\left((L-z)^2 - (a)^2\right)\right]\mathrm{d}z \tag{15}$$

The change of elastic strain energy dissipated by friction stress with respect to the crack length can then be written as:

$$\frac{\mathrm{d}U_{\mathrm{F}}}{\mathrm{d}a} = \frac{2\pi r_{\mathrm{f}}\tau}{E_{\mathrm{f}}}\left[\left(\sigma_{\mathrm{P}} - \frac{2\tau a_0}{r_{\mathrm{f}}} - \sigma_{\mathrm{fr}}^z\right)a - \frac{2\tau}{r_{\mathrm{f}}}a^2\right] \tag{16}$$

Finally, using Equation (2), the interfacial fracture toughness is derived as:

$$G_{\mathrm{Ic}} = \frac{r_{\mathrm{f}}}{4E_{\mathrm{f}}}\left[\left(\sigma_{\mathrm{p}} - \frac{2\tau a_0}{r_{\mathrm{f}}} + \nu\sigma_{\mathrm{fr}}^{\mathrm{r}} - \sigma_{\mathrm{fr}}^z - \frac{2\tau a}{r_{\mathrm{f}}}\right)^2 + (1 - \nu^2)(\sigma_{\mathrm{fr}}^{\mathrm{r}})^2 + (\sigma_{\mathrm{fr}}^z)^2\right] \tag{17}$$

In Equation (17), terms $\sigma_{\mathrm{fr}}^{\mathrm{r}}$,$\sigma_{\mathrm{fr}}^{z}$, and $\frac{2\tau a_0}{r_{\mathrm{f}}}$ are the contributions of thermal stress through different mechanisms. Therefore, the thermal residual stress should play a significant role in determining the interfacial fracture toughness. It should be noted that although the Equation (17) is obtained under the condition that the interfacial crack propagates from the bottom to top ends of the sample, it is nearly identical to the solution when the crack propagates from the bottom to top ends. Thus, Equation (17) can be generally applied to push-out test for estimation of interfacial toughness.

2.3. Finite element model

A finite element model is developed to determine the interfacial fracture toughness and validate the analytical solution described above. The finite element model is an axisymmetric cylindrical model, as shown in Figure 3(a), consisting of a SiC fiber with a radius of $r_f = 0.07$ mm and a height of $L = 0.5$ mm, and Ti-metal matrix (Timetal-834) with a radius of $r_m = 0.112$ mm. The fiber and the matrix are constructed by isoparametric four-noded quadrilateral elements while the interface is modeled with contact–friction element and spring element, as shown in Figure 3(b). The SiC fiber is treated as a perfectly isotropic elastic material and the matrix is assumed to be a rate-independent elastic–plastic material. The property's dependency on temperature is also included in the analysis and the thermo-mechanical properties of the fiber and the matrix are listed in Table 1.

The finite element analysis consists of two steps: (1) Modeling the cooling of the metal matrix composites and (2) modeling the push-out test process. When metal matrix composite is cooled from high temperature to room temperature, thermal residual stress is induced due to the mismatch of the coefficient of thermal expansion. In finite element analysis, this cooling process is modeled using thermal load, and a reference temperature (T_{ref}) is assumed above which the composites are stress free. The boundary conditions are:

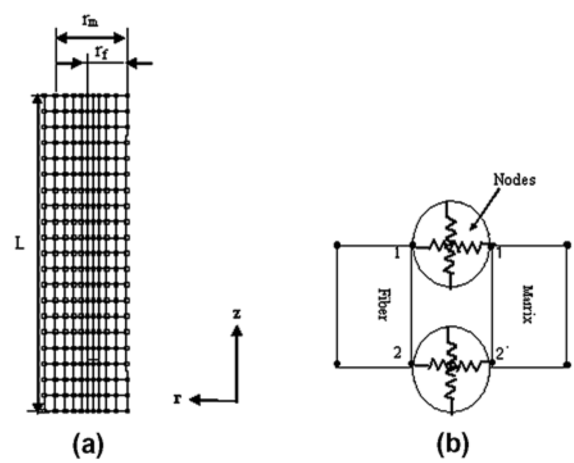

Figure 3. (a) Axisymmetric finite element model and (b) details of spring model of the interface.

Table 1. Thermo-elastic parameters of SiC and Timetal used in finite element analysis.

Material	T (°C)	E (GPa)	v	a ($\times 10^{-6}$ °C)
Timetal-834	28	115	0.3	11.24
	300	96.4	0.3	11.24
	530	84	0.3	11.24
SiC	All temperature	469	0.17	4.0

$$u_Z^{\mathrm{m}}(L/2, r) = u_Z^{\mathrm{f}}(L/2, r) = 0 \tag{18}$$

$$u_{\mathrm{r}}^{\mathrm{f}}(0, Z) = 0 \tag{19}$$

where, u_Z^{m} is the axial displacement of matrix, u_Z^{f} the axial displacement of fiber, and $u_{\mathrm{r}}^{\mathrm{f}}$ the radial displacement. In addition, the free end surface of the model can be simulated via removing the existing tying constraint and spring elements [1,21–23]. Two interfacial cracks with a length of 0.0125 mm are introduced at the two ends of the model.

For push-out test, the prescribing displacement is applied to the top end of the fiber to push the fiber out completely. A special subroutine is designed to control the interfacial failure. The interface failure process is based on strain energy failure criterion given by:

$$G \geq G_{\mathrm{Ic}} \tag{20}$$

where, G is the energy release rate of the interface crack. When the strain energy release rate of the interface crack (G) exceeds the critical value, the spring stiffness is reduced to zero and the debonding is initiated. Once the interfacial debonding occurs, the frictional sliding is introduced at the debonding interface. The frictional sliding behavior of the interface is described by the Coulomb's law:

$$\tau = \mu \sigma_{\mathrm{fr}}^{\mathrm{r}} \tag{21}$$

where, μ the coefficient of friction. In the push-out simulation, the bottom end of the matrix ($z = 0$) is fixed:

$$u_z^{\mathrm{m}}(a, r) = 0 \quad (R_{\mathrm{f}} \leq r \leq R_{\mathrm{m}}) \tag{22}$$

3. Results and discussion

3.1. *Effect of thermal stress and frictional dissipation*

Figure 4 shows the energy release rate of SiC/Timetal-834 as a function of residual stress, predicted by the finite element analysis and various analytical solutions with and without

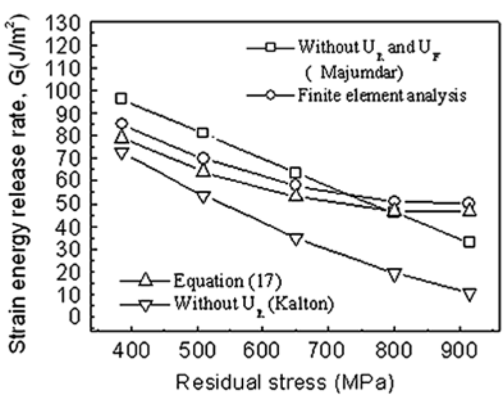

Figure 4. Energy release rate as a function of residual stress, predicted by finite element analysis and analytical solutions in the literature [14,15] and current work.

considering residual stress (U_R) and energy dissipation by friction (U_p). With increase in the residual stress, the strain energy release rate predicted by finite element analysis decreases but slows down at higher residual stress. The predictions from Equation (17) well agree with the finite element results. If the thermal strain energy U_R and the strain energy dissipated by friction stress U_F were ignored, as shown by Majumdar and Miracle for simple solution [14], the solution predicts a linear relationship between the energy release rate reduction and the residual stress. The solution without considering the residual stress energy severely underestimates the strain energy release rate. These results show that the residual stresses, the thermal strain energy dissipation by friction, and the Poisson expansion coefficient are essential factors that need to be considered in analyzing the push-out test. These factors are accounted for in our solution (Equation 17).

Our solution can also explain the effect of temperature on the critical applied stress. In the push-out test of SiC fiber-reinforced titanium matrix composites, reported by Eldridge [24] and Kalton [15], the critical applied stress increases initially as the temperature rises but it decreases with further increasing the temperature. Such an initial increase in the critical applied stress is attributed to the compensation for the reduced thermal strain energy release rate. We have calculated the strain energy release rate due to thermal residual stress (dU_R/da) and the interface friction stress (dU_F/da) by using Equation (16). In the calculation, the residual stresses versus temperature were determined by the finite element analysis, as shown in Figure 5. The energy release rate as a function of temperature is shown in Figure 6. It can be seen that below 200 °C, the decrease of thermal strain energy release rate is about 20 J/m^2, while the strain energy release rate consumed by friction stress is almost constant. Since the change of interfacial fracture toughness is small below 200 °C, according to Equation (2), the higher critical applied stress is required to offset the decrease of thermal strain energy release rate. When the temperature is above 200 °C, the decrease in thermal strain energy release rate is slowed down (only 0.04 J/m^2 °C) while the strain energy release rate dissipated by friction stress decreases quickly. As a result, a relatively low applied stress can drive the interfacial crack growth. Therefore, for titanium matrix composites, thermal strain energy release rate is an important factor for the critical applied stress in push-out test in the range of 28–200 °C while above 200 °C, the energy release rate dissipated by friction stress is a key factor for the critical applied stress.

The debonding length a, at which the applied load reaches the maximum load, may have significant effect on the interfacial energy release rate in the push-out test. According to

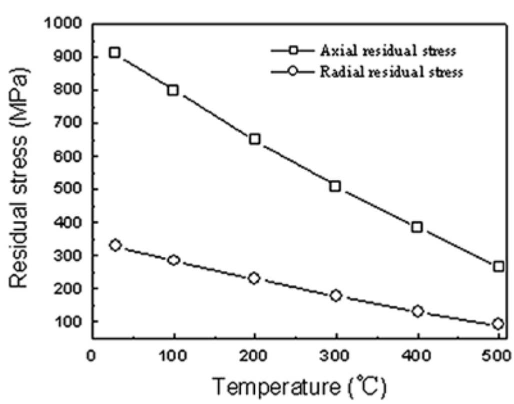

Figure 5. Axial and radial residual stresses as the function of temperature.

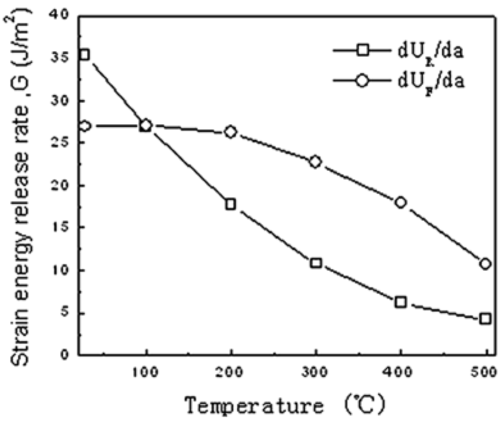

Figure 6. Strain energy release rate as a function of temperature.

Equation (17), the interfacial energy release rate of composites decreases with increasing a. Figure 7 shows the interfacial energy release rate of SiC/Timetal-834 with different debonding lengths, estimated by Equation (17). The interfacial energy release rate decreases at a rate of about 8–10 J/m^2 per 0.01 mm increase in the debonding length. Liu and Kagawa also showed that the interfacial energy release rate of ceramic matrix composites decreases with increasing the debonding length using the Lamé solution [25]. Therefore, estimation of the debonding length is important to accurately evaluate the interfacial fracture toughness.

3.2. Compression with FE and experimental results

Interfacial fracture toughness was calculated with the analytical solution (Equation (17)) and compared with finite element analysis on SiC fiber-reinforced Timetal-834. To make a comparison, the parameters required by the analytical solution, such as $\sigma_{\mathrm{fr}}^{\mathrm{r}}$, σ_{fr}^{z}, a, and τ, were also determined by the finite element analysis. Figure 8 shows the distribution of axial residual stress and radial residual stress in the fiber of SiC/Timetal-834, which gives an axial residual stress of σ_{fr}^{z} = 914 MPa and a radial residual stress of $\sigma_{\mathrm{fr}}^{\mathrm{r}}$ = 330 MPa. According to experimental results on SiC fiber-reinforced timetal-834 [1], the coefficient of friction is $\mu = 0.4$, yielding an interface frictional stress of $\tau = 132$ MPa. A crack length of $a = 0.15$ mm at

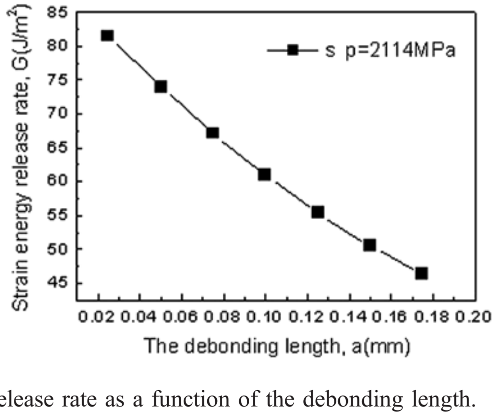

Figure 7. Strain energy release rate as a function of the debonding length.

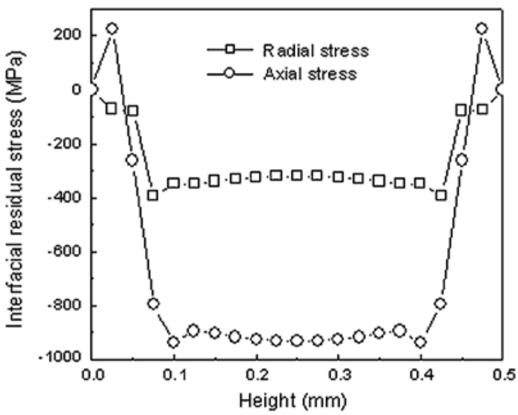

Figure 8. The distribution of residual stress in the fiber along the axial coordinate.

maximum applied load was also reported [1]. These parameters used the analysis that are summarized and listed in Table 2. Using these parameters, the interfacial fracture toughness of SiC fiber-reinforced Timetal-834 was calculated to be about 46.21 J/m^2.

Next, interfacial fracture toughness was directly computed by using the finite element analysis. Using the same parameters listed in Table 2, we obtain the critical energy release rate to be 50 J/m^2, very close the analytical results. This result is consistent with the finite element analysis for SCS-6/Timetal-21 made by Mukherjee and Miracle [17]. In their analysis, an interfacial energy release rate of 54 J/m^2 was reported. It should be noted that the load–displacement curves predicted by our finite element analysis are also in good agreement with the experiment results, as shown in Figure 9. In addition, our analytical and numerical analyses

Table 2. Parameters used to examine predictions of the analytical model.

E_f (GPa)	r_f (μm)	σ_{fr}^{z} (MPa)	σ_{fr}^{r} (MPa)	τ (MPa)	σ_p (MPa)	a (μm)	a_0 (μm)
469	70	914	330	132	2014	12.5	150

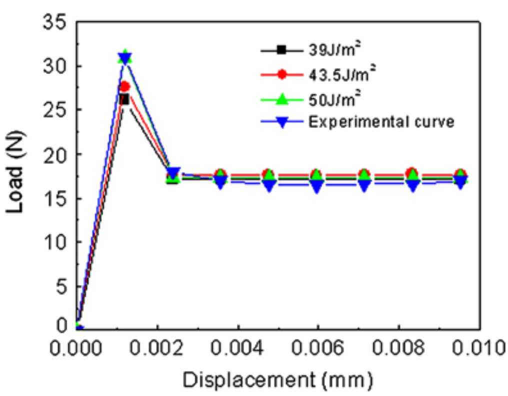

Figure 9. The load–displacement curves of push-out test by finite element method and experiment [1] ($\mu = 0.4$).

show that the thermal residual stress plays an essential role in determining the interfacial fracture toughness. Without considering the thermal stress, the interfacial strain energy release rate predicted by the analytical solution is 11 J/m^2, while the thermal strain energy release rate is 35 J/m^2. This indicates that most of the energy contribution to the failure process comes from the residual stress [15,17]. The analytical model does predict the importance of the thermal stress in determining the interfacial fracture toughness.

4. Conclusions

An analytical model was developed to predict the interfacial fracture toughness of fiber-reinforced matrix composites in push-out test. Thermal residual stress, Poisson effect, frictional force, and interfacial friction energy dissipation are all considered in the analytical model. Finite element models are also developed to validate the analytical solution. The interfacial fracture toughness of SiC/Timetal-834 predicted by the analytical model is 46.7 J/m^2, very close to the finite element predictions and experimental results. The analytical results also show a high thermal strain energy release rate of 35 J/m^2, about 75% of the interfacial fracture toughness, suggesting that most of the energy contribution to the failure process comes from the residual stress in SiC/Timetal-834 composites. The analytical model successfully explains the unusual phenomena in high-temperature push-out tests on SiC fiber-reinforced titanium matrix composites, in which the critical applied stress initially increases, and then decreases with increasing temperature.

Acknowledgments

We would like to acknowledge the support of the Chinese Education Ministry Foundation for Doctors (20101420120006) and the Doctoral Foundation of Northwestern Polytechnical University (BP201004), the Natural Science Foundation of China (51201155) and the ‘111’ Program for Cooperation.

References

[1] Zeng WD, Peters PWM, Tanaka Y. Interfacial bond strength and fracture energy at room and elevated temperature in titanium matrix composites (SCS-6/Timetal 834). Composites: Part A. 2002;33:1159–1170.
[2] Gundel DB, Warrier SG, Miracle DB. The interface debond stress in single and multiple SiC fiber/Ti-6Al-4V composites under transverse tension. Acta Mater. 1997;45:1275–1284.
[3] Yang YQ, Dudek HJ, Kumpfert J. Interface stability in SCS-6 SiC/Super α_2 composites. Scripta Mater. 1997;37:503–510.
[4] Fukushima A, Fujiwara C, Kagawa Y, Masuda C. Effect of interfacial properties on tensile strength in SiC/Ti-15-3 composites. Mater. Sci. Eng., A. 2000;276:243–249.
[5] Bouazaoui L, Li A. Analysis of steel/concrete interfacial shear stress by means of pull out test. Int. J. Adhes. Adhes. 2008;28:101–108.
[6] Tandon GP, Pagano NJ. Micromechanical analysis of the fiber push-out and re-push test. Compos. Sci. Technol. 1998;58:1709–1725.
[7] Andersons J, Leterrier Y, Tornare G, Dumont P. Evaluation of interfacial stress transfer efficiency by coating fragmentation test. Mech. Mater. 2007;39:834–844.
[8] Kallas MN, Koss DA, Hahn HT, Hellman JR. Interfacial stress state present in a thin slice push out test. J. Mater. Sci. 1992;27:3821–3826.
[9] Zhou LM, Kim JK, Mai YW. Micromechanical characterization of fibre/matrix interfaces. Compos. Sci. Technol. 1993;48:227–236.
[10] Zhou LM, Mai YW. Analysis of fiber push out test based on the fracture mechanics approach. Compos. Eng. 1995;5:1199–1219.
[11] Hsuech CH. Evaluation of interfacial shear strength, residual clamping stress and coefficient of friction for fiber-reinforced ceramic composites. Acta Metall. Mater. 1990;38:403–409.

[12] Hsuech CH, Rebillat F, Lamon J, Lara-Curzio E. Analyses of fiber push-out tests performed on Nicalon/SiC composites with tailored interface. Compos. Eng. 1995;5:1387–1401.
[13] Parthasarathy TA, Barlarge DB, Jero PD, Kerans RJ. Effect of interfacial roughness parameters on the fiber push out behavior of model composite. J. Am. Ceram. Soc. 1994;77:3232–3236.
[14] Majumdar BS, Miracle DB. Interface measurements and application in fiber reinforced MMCs. Key Eng. Mater. 1996;116:153–172.
[15] Kalton AF, Howard SJ, Janczak J, Clyne TW. Measurement of interfacial fracture energy by single fiber push out testing and its application to the titanium silicon carbide system. Acta Mater. 1998;46:3175–3189.
[16] Huang B, Yang YQ, Luo HJ. Effect of the interfacial reaction layer thickness on the thermal residual stresses in SiC_f/Ti–6Al–4V composites. Mater. Sci. Eng., A. 2008;48:178–186.
[17] Mukherjee S, Ananth CR, Chandra N. Evaluation of fracture toughness of MMC interfaces using thin-slice push out tests. Scripta Mater. 1997;36:1333–1338.
[18] Hutchinson JW. Models of fiber debonding and pullout in brittle composites with friction. Mech. Mater. 1990;9:139–163.
[19] Parthasarathy TA, Marshall DB, Kerans RJ. Analysis of the effect of interfacial roughness on fiber debonding and sliding in brittle matrix composites. Acta Metall. Mater. 1994;42:3773–3784.
[20] Gao YC, Mai YW, Cotterell B. Fracture of fiber-reinforced materials. Z. Angew. Math. Phys. (ZAMP). 1988;39:550–572.
[21] Yuan MN, Yang YQ. Analysis of interfacial behavior in titanium matrix composites by using the finite element method (SCS-6/Ti55). Scripta Mater. 2007;56:533–536.
[22] Ananth CR, Chandra N. Elevated temperature interfacial behaviour of MMCs: a computational study. Composites: Part A. 1996;27:805–811.
[23] Chandra N, Ananth CR. Analysis of interfacial behaviour in MMCs and IMCs by the use of thin slice push-out tests. Compos. Sci. Technol. 1995;54:87–100.
[24] Eldridge JI, Ebihara BT. Fiber push-out testing apparatus for elevated temperatures. J. Mater. Res. 1994;9:1035–1042.
[25] Liu YF, Kagawa Y. The energy release rate for an interfacial debond crack in a fiber pull-out model. Compos. Sci. Technol. 2000;60:167–171.